

Short Communication

The preparation and electrochemical performance of Lu³⁺/Gd³⁺ co-doped ceria-chloride composite electrolyte

Jilong Ma*, Mengjuan Zhang, Lili Wang, Xiangsong Meng, Wenjian Wang, Jian Tang, Guoquan Shao*

College of Traditional Chinese Medicine, Bozhou University, Bozhou Anhui 236800, China

*E-mail: bxymjl2019@163.com

Received: 1 October 2020 / Accepted: 16 November 2020 / Published: 30 November 2020

In this study, Ce_{0.8}Gd_{0.1}Lu_{0.1}O_{2-α} was synthesized by a sol-gel method. And Ce_{0.8}Gd_{0.1}Lu_{0.1}O_{2-α}-(Na/K)Cl composite electrolyte was prepared at 750 °C. The phase composition, microstructure, conductivity and fuel cell properties of the composite were studied at 500–750 °C. The XRD results showed that no chemical reaction occurred between chloride and Ce_{0.8}Gd_{0.1}Lu_{0.1}O_{2-α}. The log σ ~ log (pO₂) results showed that Ce_{0.8}Gd_{0.1}Lu_{0.1}O_{2-α}-(Na/K)Cl is a pure ionic conductor in an oxidizing atmosphere. The performance of oxygen concentration discharge cell further showed that Ce_{0.8}Gd_{0.1}Lu_{0.1}O_{2-α}-(Na/K)Cl is an excellent oxygen ion conductor in an oxidizing atmosphere.

Keywords: Composite; Electrolyte; Fuel cell; CeO₂; Conductivity

1. INTRODUCTION

A fuel cell is a kind of power generation device which can convert chemical energy stored in fuel and oxidant into electric energy with high efficiency. Fuel cells can be classified according to their operating temperatures or electrolytes. A solid electrolyte is the core component of a solid oxide fuel cell (SOFC) [1-6]. The traditional high-temperature SOFC (800–1000 °C) uses Y₂O₃ stabilized zirconia (YSZ) as the electrolyte. Such a high operating temperature causes a series of problems. An effective way to reduce the working temperature of an SOFC is to find an electrolyte with high ionic conductivity at medium temperature (400–700 °C) [7-11].

The ionic conductivities of CeO₂-based materials with a cubic structure are higher than that of YSZ at medium temperature (400–700 °C) [12-16]. Tian et al. synthesized Sm_{0.15}Ce_{0.85}O_{2-δ} using 0.5mol% CuO as a sintering aid [12]. The oxygen vacancy concentrations in the lattice increased and the oxygen ion conductivities improved, while two kinds of low valence metal ions replaced Ce⁴⁺ [17-21]. Soepriyanto et al. found that Gd³⁺ and Nd³⁺ co-doped CeO₂ had higher conductivities than Gd³⁺ and Y³⁺ co-doped CeO₂ [20]. The traditional solid-state method of CeO₂-based electrolytes requires a high

sintering temperature. In order to obtain uniform nanoscale powders at low temperature, $\text{Ce}_{0.8}\text{Gd}_{0.1}\text{Lu}_{0.1}\text{O}_{2-\alpha}$ was synthesized by a sol-gel method in this study.

However, part of Ce^{4+} is reduced to Ce^{3+} in a reductive atmosphere. In the research on medium temperature SOFCs, it is of great significance to develop new composite electrolyte materials with high conductivities [22-25]. Kumar et al. combined $\text{Sm}^{3+}/\text{Gd}^{3+}$, $\text{Sr}^{2+}/\text{Gd}^{3+}$ and $\text{Ca}^{2+}/\text{Gd}^{3+}$ co-doped ceria with Na_2CO_3 to synthesize nanocomposite electrolytes [22]. Therefore, it is of great significance to explore new types of Gd^{3+} and Lu^{3+} co-doped ceria-chloride composite electrolytes for the development of medium temperature SOFCs.

In this study, $\text{Ce}_{0.8}\text{Gd}_{0.1}\text{Lu}_{0.1}\text{O}_{2-\alpha}$ was synthesized by a sol-gel method. And $\text{Ce}_{0.8}\text{Gd}_{0.1}\text{Lu}_{0.1}\text{O}_{2-\alpha}$ -(Na/K)Cl composite electrolyte was prepared at 750 °C. The phase composition, microstructure, conductivity and fuel cell properties of the composite were studied at 500–750 °C.

2. EXPERIMENTAL

$\text{Ce}_{0.8}\text{Gd}_{0.1}\text{Lu}_{0.1}\text{O}_{2-\alpha}$ was prepared using a sol-gel method. Firstly, Gd_2O_3 (99.99%) and Lu_2O_3 (99.99%) were dissolved using nitric acid, and mixed with $(\text{NH}_4)_2\text{Ce}(\text{NO}_3)_6$ (99.9%) solution. The citric acid was added with a molar weight 1.5 times that of the metal cations. The solution was stirred and evaporated until the gel formed. After removal of residual organic matter, the powder was put into a muffle furnace and calcined at 900 °C for 5 h to obtain $\text{Ce}_{0.8}\text{Gd}_{0.1}\text{Lu}_{0.1}\text{O}_{2-\alpha}$. The $\text{Ce}_{0.8}\text{Gd}_{0.1}\text{Lu}_{0.1}\text{O}_{2-\alpha}$ powder was mixed with melted NaCl-KCl powder in the mass ratio of 3:1. The fully grinded powder was pressed into a disc with a diameter of 18 mm at 250 MPa. $\text{Ce}_{0.8}\text{Gd}_{0.1}\text{Lu}_{0.1}\text{O}_{2-\alpha}$ -(Na/K)Cl composite electrolyte was prepared after being heated at 750 °C for 1 h.

The thermogravimetry analysis and differential scanning calorimetry (TGA-DSC, Universal V 3.7A, TA Instruments, USA) curve of xerogel was measured by a thermogravimetric analyser. The phases of the $\text{Ce}_{0.8}\text{Gd}_{0.1}\text{Lu}_{0.1}\text{O}_{2-\alpha}$ and $\text{Ce}_{0.8}\text{Gd}_{0.1}\text{Lu}_{0.1}\text{O}_{2-\alpha}$ -(Na/K)Cl powders were determined by X-ray diffractometer (XRD, X'pert Pro MPD, Netherlands). The microstructure of $\text{Ce}_{0.8}\text{Gd}_{0.1}\text{Lu}_{0.1}\text{O}_{2-\alpha}$ -(Na/K)Cl was observed by a scanning electron microscope (SEM, S-4700, Hitachi, Japan). The sintered disc of $\text{Ce}_{0.8}\text{Gd}_{0.1}\text{Lu}_{0.1}\text{O}_{2-\alpha}$ -(Na/K)Cl was processed into a thin sheet with an electrode diameter of 8 mm (area: 0.5 cm²) and a thickness of 1.0 mm, which was used for gas concentration cell, conductivity and fuel cell.

3. RESULTS AND DISCUSSION

The TGA-DSC curve of xerogel ($\text{Ce}_{0.8}\text{Gd}_{0.1}\text{Lu}_{0.1}\text{O}_{2-\alpha}$) from room temperature to 900 °C in a nitrogen atmosphere is shown in Fig. 1. As shown in Fig. 1, the continuous mass loss of the xerogel ranges from room temperature to 300 °C and the total mass loss was about 80%. On the DSC curve, there is an obvious exothermic peak near 260 °C, accompanied by about 65 % mass loss, which was mainly caused by the decomposition of nitrate and citrate [18-19]. When the temperature was higher than 600 °C, no obvious mass loss was observed on the TG curve, and the DSC curve becomes flatter,

indicating that the decomposition, oxidation and crystallization process of xerogel were basically complete [21]. Therefore, the calcination temperature should be above 600 °C.

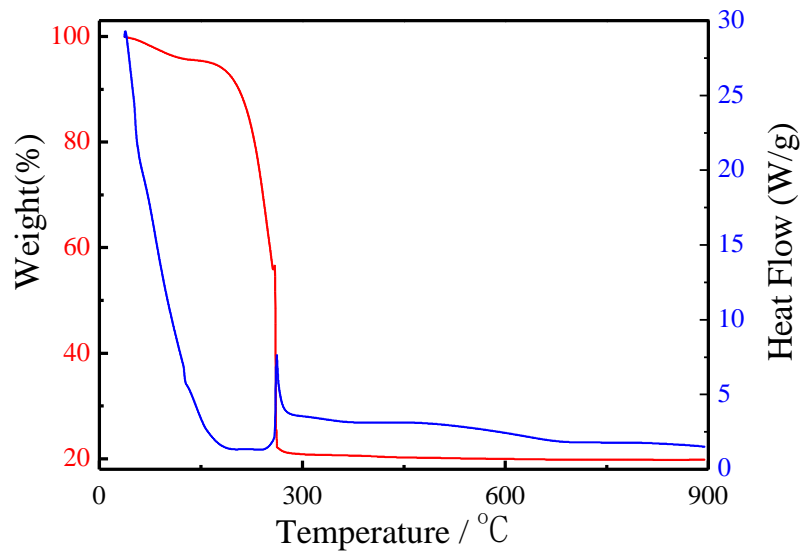


Figure 1. TGA-DSC curve of xerogel ($\text{Ce}_{0.8}\text{Gd}_{0.1}\text{Lu}_{0.1}\text{O}_{2-\alpha}$) from room temperature to 900 °C in a nitrogen atmosphere.

Fig. 2 is the XRD diagram of $\text{Ce}_{0.8}\text{Gd}_{0.1}\text{Lu}_{0.1}\text{O}_{2-\alpha}$ and $\text{Ce}_{0.8}\text{Gd}_{0.1}\text{Lu}_{0.1}\text{O}_{2-\alpha}-(\text{Na/K})\text{Cl}$ powders. It can be seen from Fig. 2 that the $\text{Ce}_{0.8}\text{Gd}_{0.1}\text{Lu}_{0.1}\text{O}_{2-\alpha}$ powder calcined at 900 °C has a single cubic fluorite structure, and no other impurity diffraction peaks are found [17-19]. It is indicated that Gd^{3+} and Lu^{3+} enter the CeO_2 lattice in the form of Ce^{4+} instead, indicating that the sol-gel method is suitable for preparing multi component CeO_2 electrolyte powders [21]. In the composite electrolyte, there are some crystal phases of NaCl and KCl in the chloride phase. $\text{Ce}_{0.8}\text{Gd}_{0.1}\text{Lu}_{0.1}\text{O}_{2-\alpha}$ still keeps its original lattice structure and does not react with chloride, which indicates that $\text{Ce}_{0.8}\text{Gd}_{0.1}\text{Lu}_{0.1}\text{O}_{2-\alpha}$ particles have good corrosion resistance [23-24].

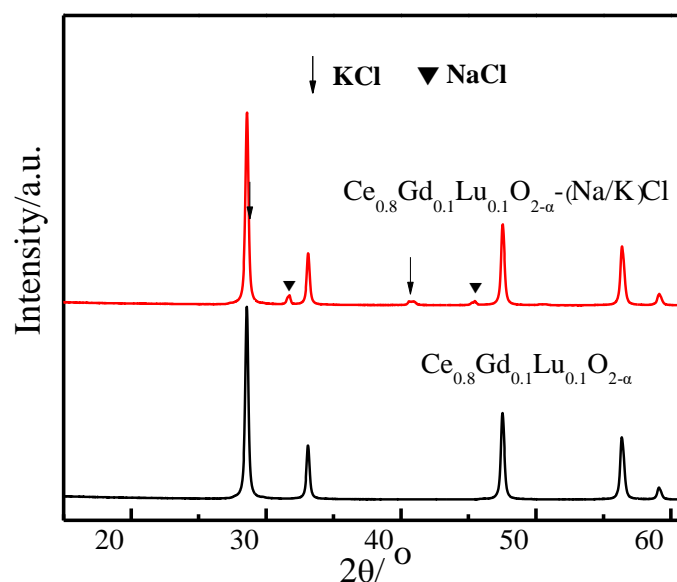


Figure 2. XRD patterns of $\text{Ce}_{0.8}\text{Gd}_{0.1}\text{Lu}_{0.1}\text{O}_{2-\alpha}$ and $\text{Ce}_{0.8}\text{Gd}_{0.1}\text{Lu}_{0.1}\text{O}_{2-\alpha}-(\text{Na/K})\text{Cl}$ powders.

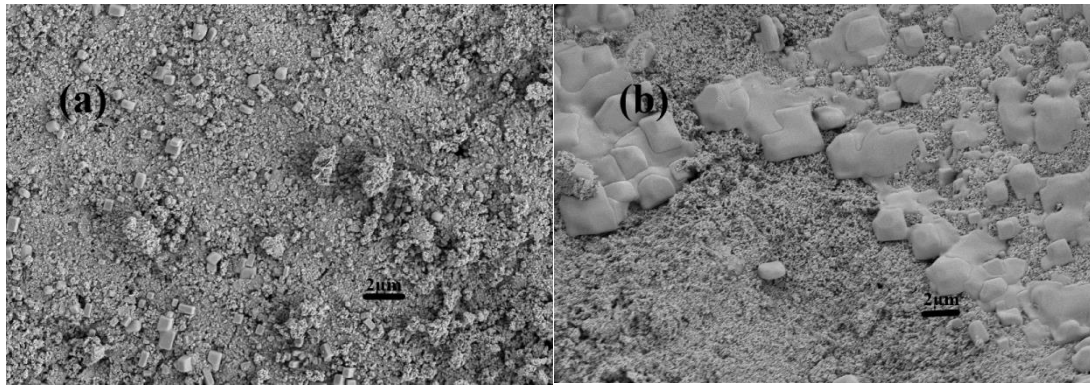


Figure 3. The SEM photos of $\text{Ce}_{0.8}\text{Gd}_{0.1}\text{Lu}_{0.1}\text{O}_{2-\alpha}-(\text{Na/K})\text{Cl}$ (a) external, (b) cross-sectional.

Figure 3 shows the SEM photos of $\text{Ce}_{0.8}\text{Gd}_{0.1}\text{Lu}_{0.1}\text{O}_{2-\alpha}-(\text{Na/K})\text{Cl}$ calcined at $900\text{ }^\circ\text{C}$ for 5 h. The morphology of $\text{Ce}_{0.8}\text{Gd}_{0.1}\text{Lu}_{0.1}\text{O}_{2-\alpha}$ remains basically as spherical nanoparticles, from Fig. 3 (a). From Fig. 3 (b), in the composite, due to the small size of $\text{Ce}_{0.8}\text{Gd}_{0.1}\text{Lu}_{0.1}\text{O}_{2-\alpha}$ particles, chloride phase can be seen on the surface of $\text{Ce}_{0.8}\text{Gd}_{0.1}\text{Lu}_{0.1}\text{O}_{2-\alpha}$ particles [22]. It can be seen from Fig. 3 that the $\text{Ce}_{0.8}\text{Gd}_{0.1}\text{Lu}_{0.1}\text{O}_{2-\alpha}$ and $(\text{Na/K})\text{Cl}$ phases prepared by sol-gel method are evenly distributed after being sintered at $900\text{ }^\circ\text{C}$ for 5 h [24].

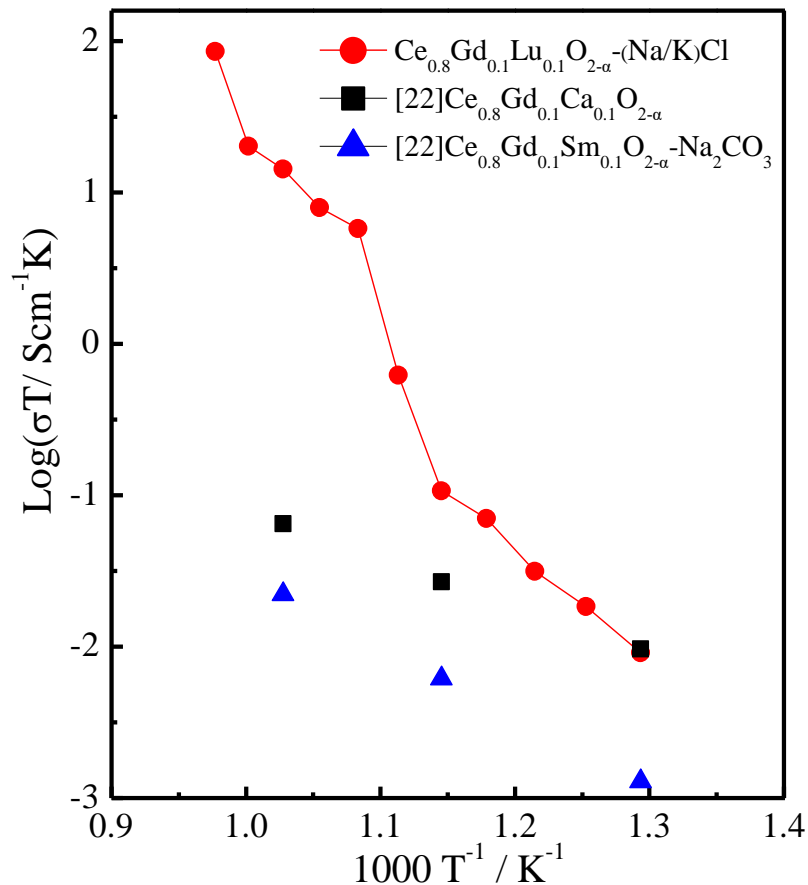


Figure 4. The conductivities of $\text{Ce}_{0.8}\text{Gd}_{0.1}\text{Lu}_{0.1}\text{O}_{2-\alpha}-(\text{Na/K})\text{Cl}$ from 500 to $750\text{ }^\circ\text{C}$ in nitrogen.

Fig. 4 shows the AC conductivity test results of $\text{Ce}_{0.8}\text{Gd}_{0.1}\text{Lu}_{0.1}\text{O}_{2-\alpha}(\text{Na/K})\text{Cl}$ from 500 to 750 °C in nitrogen. In the range of 500–600 °C, the conductivity of the composite electrolyte is one order of magnitude higher than that Kumar et al. reported for $\text{Ce}_{0.8}\text{Gd}_{0.1}\text{Ca}_{0.1}\text{O}_{2-\alpha}$ [22]. There is a turning point in the conductivity of $\text{Ce}_{0.8}\text{Gd}_{0.1}\text{Lu}_{0.1}\text{O}_{2-\alpha}(\text{Na/K})\text{Cl}$ near the melting temperature of the chloride phase, and the activation energy changes significantly near this temperature. In the molten state (600–700 °C), the AC conductivity of $\text{Ce}_{0.8}\text{Gd}_{0.1}\text{Lu}_{0.1}\text{O}_{2-\alpha}(\text{Na/K})\text{Cl}$ is higher than $\text{Ce}_{0.8}\text{Gd}_{0.1}\text{Ca}_{0.1}\text{O}_{2-\alpha}$ [22] by 2.5 orders of magnitude. At the same time, the conductivity of $\text{Ce}_{0.8}\text{Gd}_{0.1}\text{Lu}_{0.1}\text{O}_{2-\alpha}(\text{Na/K})\text{Cl}$ ($8.3 \times 10^{-2} \text{ S} \cdot \text{cm}^{-1}$) is higher than that of $\text{Ce}_{0.8}\text{Gd}_{0.1}\text{Sm}_{0.1}\text{O}_{2-\alpha}\text{-Na}_2\text{CO}_3$ [22]. In conclusion, the appropriate proportion of Gd^{3+} and Lu^{3+} doping can effectively improve the conductivity of CeO_2 -based composite electrolyte materials.

Fig. 5 shows the curves of conductivities changing with oxygen content. The $\log \sigma \sim \log (p\text{O}_2)$ curve of $\text{Ce}_{0.8}\text{Gd}_{0.1}\text{Lu}_{0.1}\text{O}_{2-\alpha}(\text{Na/K})\text{Cl}$ is higher than that of $\text{Ce}_{0.8}\text{Gd}_{0.1}\text{Yb}_{0.1}\text{O}_{2-\alpha}$ and close to that of $\text{Ce}_{0.8}\text{Gd}_{0.1}\text{Yb}_{0.1}\text{O}_{2-\alpha}\text{-KCl-NaCl}$ reported by Wang et al. [26]. The conductivities do not change with the ratio of gas (nitrogen and oxygen), showing a horizontal line. The results show that $\text{Ce}_{0.8}\text{Gd}_{0.1}\text{Lu}_{0.1}\text{O}_{2-\alpha}(\text{Na/K})\text{Cl}$ is a pure ionic conductor in an oxidizing atmosphere.

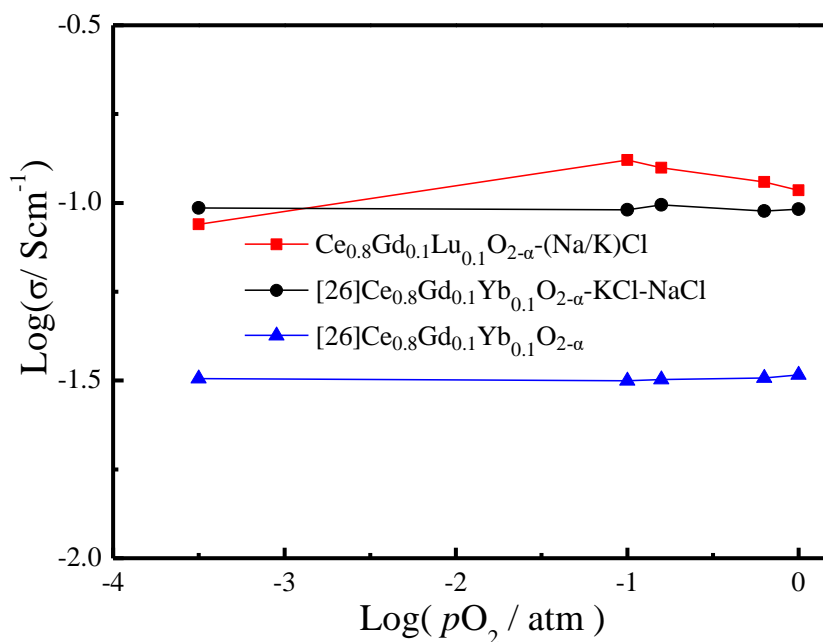


Figure 5. The $\log \sigma \sim \log (p\text{O}_2)$ curve of $\text{Ce}_{0.8}\text{Gd}_{0.1}\text{Lu}_{0.1}\text{O}_{2-\alpha}(\text{Na/K})\text{Cl}$.

The performance of oxygen concentration discharge cell using $\text{Ce}_{0.8}\text{Gd}_{0.1}\text{Lu}_{0.1}\text{O}_{2-\alpha}(\text{Na/K})\text{Cl}$ as electrolyte at 750 °C is shown in Fig. 6. The open circuit voltage (34 mV) is in agreement with the theoretical value (34.4 mV). When the current density is $1.25 \text{ mA} \cdot \text{cm}^{-2}$, the power density reaches the maximum value of $0.024 \text{ mW} \cdot \text{cm}^{-2}$. Combined with the conclusion in Fig. 5, the results further show that $\text{Ce}_{0.8}\text{Gd}_{0.1}\text{Lu}_{0.1}\text{O}_{2-\alpha}(\text{Na/K})\text{Cl}$ is an excellent oxygen ion conductor in an oxidizing atmosphere.

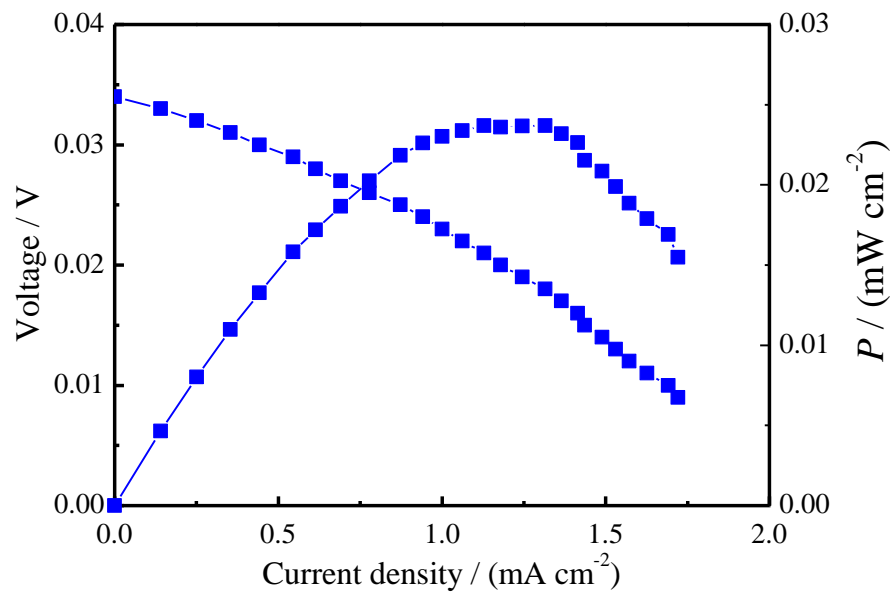


Figure 6. The performance of oxygen concentration discharge cell using $\text{Ce}_{0.8}\text{Gd}_{0.1}\text{Lu}_{0.1}\text{O}_{2-\alpha}(\text{Na/K})\text{Cl}$ as electrolyte at $750\text{ }^{\circ}\text{C}$.

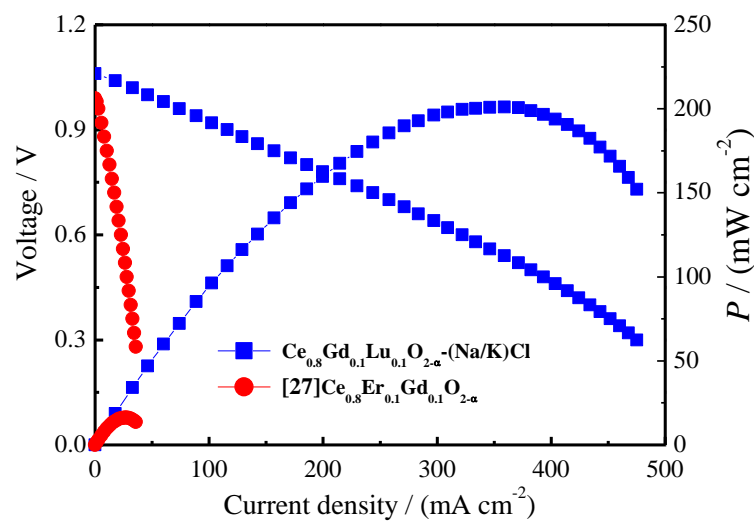


Figure 7. The performance of oxygen/hydrogen fuel cell using $\text{Ce}_{0.8}\text{Gd}_{0.1}\text{Lu}_{0.1}\text{O}_{2-\alpha}(\text{Na/K})\text{Cl}$ as electrolyte at $750\text{ }^{\circ}\text{C}$.

Hydrogen is used as fuel gas and oxygen as oxidant, and the I - V - P relationship is tested. The results are shown in Fig. 7. At $750\text{ }^{\circ}\text{C}$, the open circuit voltage of $\text{Ce}_{0.8}\text{Gd}_{0.1}\text{Lu}_{0.1}\text{O}_{2-\alpha}(\text{Na/K})\text{Cl}$ is 1.06 V , which is close to the theoretical value, indicating that the composite electrolyte synthesized above the eutectic temperature is dense. For a single CeO_2 electrolyte ($\text{Ce}_{0.8}\text{Er}_{0.1}\text{Gd}_{0.1}\text{O}_{2-\alpha}$ reported by Zhang et al. [27]), the open circuit voltage is 0.98 V due to the conversion of part of Ce^{4+} to Ce^{3+} in a reducing atmosphere. Therefore, the addition of a certain amount of chloride in the composite electrolyte can effectively inhibit the electron conduction of $\text{Ce}_{0.8}\text{Gd}_{0.1}\text{Lu}_{0.1}\text{O}_{2-\alpha}$. When the current density is $359\text{ mA}\cdot\text{cm}^{-2}$, the power density of $\text{Ce}_{0.8}\text{Gd}_{0.1}\text{Lu}_{0.1}\text{O}_{2-\alpha}(\text{Na/K})\text{Cl}$ reaches the maximum value of $201\text{ mW}\cdot\text{cm}^{-2}$ at $750\text{ }^{\circ}\text{C}$.

4. CONCLUSIONS

In this study, $\text{Ce}_{0.8}\text{Gd}_{0.1}\text{Lu}_{0.1}\text{O}_{2-\alpha}(\text{Na/K})\text{Cl}$ composite electrolyte was prepared at 750 °C. The TGA-DSC curve indicated that the decomposition, oxidation and crystallization process of xerogel are basically completed below 600 °C and the calcination temperature should be above 600 °C. At 750 °C, the conductivity of $\text{Ce}_{0.8}\text{Gd}_{0.1}\text{Lu}_{0.1}\text{O}_{2-\alpha}(\text{Na/K})\text{Cl}$ reached $8.3 \times 10^{-2} \text{ S} \cdot \text{cm}^{-1}$. The $\log \sigma \sim \log (p\text{O}_2)$ and oxygen concentration discharge cell results showed that $\text{Ce}_{0.8}\text{Gd}_{0.1}\text{Lu}_{0.1}\text{O}_{2-\alpha}(\text{Na/K})\text{Cl}$ is an excellent oxygen ion conductor in an oxidizing atmosphere. When the current density was $359 \text{ mA} \cdot \text{cm}^{-2}$, the power density of $\text{Ce}_{0.8}\text{Gd}_{0.1}\text{Lu}_{0.1}\text{O}_{2-\alpha}(\text{Na/K})\text{Cl}$ reached the maximum value of $201 \text{ mW} \cdot \text{cm}^{-2}$ at 750 °C.

ACKNOWLEDGEMENTS

This work was supported by the Natural Science Project of Anhui Province (No. KJ2019A1304, KJ2019ZD80), High level teaching team of Anhui Provincial Department of Education (No. 2018jxtd079, 2019jxtd131).

CONFLICTS OF INTEREST

The authors declare no conflicts of interest.

References

1. Y. Yang, H. Hao, L. Zhang, C. Chen, Z. Luo, Z. Liu, Z. Yao, M. Cao and H. Liu, *Ceram. Int.*, 44 (2018) 11109.
2. Y. Tian, Z. Lü, X. Guo and P. Wu, *Int. J. Electrochem. Sci.*, 14 (2019) 1093.
3. C. Xia, Z. Qiao, C. Feng, J. Kim, B. Wang and B. Zhu, *Materials*, 11(2018) 40.
4. X. Fang, J. Zhu and Z. Lin, *Energies*. 11 (2018) 1735.
5. Z. Zhang, L. Chen, Q. Li, T. Song, J. Su, B. Cai, H. He, *Solid State Ionics*, 323 (2018) 25.
6. A.A. Solovyev, S.V. Rabotkin, A.V. Shipilova and I.V. Ionov, *Int. J. Electrochem. Sci.*, 14 (2019) 575.
7. W. Wang, D. Medvedev and Z. Shao, *Adv. Funct. Mater.*, (2018) 1802592.
8. H. Jiang and F. Zhang, *Int. J. Electrochem. Sci.*, 15 (2020) 959.
9. W. Wang, D. Medvedev and Z. Shao, *Adv. Funct. Mater.*, 2018, 1802592.
10. S.H. Morejudo, R. Zanón, S. Escolástico, I. Yuste-Tirados, H. Malerød-Fjeld, P.K. Vestre, W.G. Coors, A. Martínez, T. Norby, J.M. Serra and C. Kjøseth, *Science*, 353 (2016) 563.
11. G. Yang and S.-J. Park, *Materials*, 12 (2019) 1177.
12. N. Tian, Y. Qu, H. Men, J. Yu, X. Wang and J. Zheng, *Solid State Ionics*, 351 (2020) 115331.
13. L. dos Santos-Gómez, J. Zamudio-García, J.M. Porrás-Vázquez, E.R. Losilla and D. Marrero-López, *J. Eur. Ceram. Soc.*, 40 (2020) 3080.
14. A. Arabaci, *Emerg. Mater. Res.*, 9 (2020) 296.
15. I. Shajahan, J. Ahn, P. Nair, S. Mediseti, S. Patil, V. Niveditha, G.U.B. Babu, H.P. Dasari and Jong-Ho Lee, *Mater. Chem. Phys.*, 216 (2018) 136.
16. Y. Itagaki, J. Cui, N. Ito, H. Aono and H. Yahiro, *J. Ceram. Soc. Jpn*, 126 (2018) 870-876.
17. Y. Jiang, H. Huang, M. Wang, W. Zhang and B. Wang, *J. Mater. Sci.*, 31 (2020) 6233.
18. Z. Huang, L. Fan, N. Hou, T. Gan, J. Gan, Y. Zhao and Y. Li, *J. Power Sources*, 451 (2020) 227809.
19. V. Vijaykumar, G. Nirala, D. Yadav, U. Kumar and S. Upadhyay, *Int. J. Energy Res.*, 44 (2020) 4652.
20. S. Soepriyanto, Y. Aristanti, T. Theresia, M. A. Sulthon, F. Baqir, W. P. Minwal and B. Dilasari, *J.*

- Aust. Ceram. Soc.*, 55 (2019) 1161.
21. J. Cheng, C. Tian and J. Yang, *J. Mater. Sci.*, 30 (2019) 16613.
 22. S.A. Kumar, P. Kuppusami, B. Vigneshwaran and Y.-P. Fu, *ACS Appl. Nano Mater.*, 2 (2019) 6300.
 23. M. Anwar, S.A.M. Ali, A. Muchtar and M.R. Somalu, *J. Alloy. Compound.*, 775 (2019) 571.
 24. S. Shawuti and M.A. Gulgun, *J. Power Sources*, 267 (2014) 128.
 25. B. Zhu, S. Li and B.E. Mellander, *Electrochem. Commun.*, 10 (2008) 302.
 26. H. Wang, T. Hu and G. Xi, *Ceram. Int.*, 46 (2020) 8695.
 27. W. Zhang, T. Hu, R. Shi and H. Wang, *Int. J. Electrochem. Sci.*, 15 (2020) 304.

© 2021 The Authors. Published by ESG (www.electrochemsci.org). This article is an open access article distributed under the terms and conditions of the Creative Commons Attribution license (<http://creativecommons.org/licenses/by/4.0/>).